Advanced Integrated Modeling and Analysis for Adjustable Speed Drives of Induction Motors Operating With Minimum Losses

Antonio T. Alexandridis, *Member, IEEE*, George C. Konstantopoulos, *Member, IEEE*, and Qing-Chang Zhong, *Senior Member, IEEE*

***Abstract*—The nonlinear induction motor model is appropriately integrated by incorporating the dynamics of the power electronic converter in a manner that permits the design of stable field-oriented control (FOC) operating with minimum losses. As already proven, the challenging issue of operating the induction machine with minimum copper losses requires a varying rotor flux opposed to the standard FOC technique, which keeps the rotor field magnitude constant and tracks the electric torque to the desired level. To this end, exploiting the Hamiltonian structure of the developed motor/converter model, an innovated nonlinear controller is proposed that guarantees the technical limits of the converter (linear modulation) and simultaneously operates under FOC at steady state to achieve accurate speed regulation with varying rotor flux according to the minimal losses requirements. Under these circumstances, the conventional FOC stability analysis does not hold anymore, and therefore for the first time, a new rigorous analysis is provided that proves stability and convergence to the desired equilibrium for the complete closed-loop motor converter system. Finally, the theoretical contribution is examined in comparison to the traditional FOC operation by simulations obtained for an industrial size induction motor, while it is further evaluated by real-time results of a motor with similar parameters.**

***Index Terms*—Converter-machine modeling, induction motor, minimum losses, nonlinear control, stability.**

I. Introduction

THE THREE-PHASE induction motor represents one of the most commonly used electric machines in industrial applications. The integration of suitable power electronic devices, particularly ac/dc voltage source converters (VSC), have decisively increased the area of applications for the induction machine and has opened a new field in design and analysis. Vector or field-oriented control (FOC), though complex and demanding technique, remains a powerful tool for adjustable induction motor speed drives [1], [2], since it results in constant rotor flux magnitude that simplifies the electromagnetic torque expression as in a separately excited dc motor. On the other hand, the motor efficiency enhancement, resulting from the reduction of copper losses, has become a crucial operating task caused by environmental or special application reasons such as wind turbine or electric vehicle efficient operation [3]–[9]. As it has been shown [10]–[17], power losses minimization certainly requires a varying rotor flux magnitude in accordance to the particular operating point.

Additionally, in all induction motor applications, stability plays a crucial role in system operation and should be always guaranteed. Several researchers have proposed FOC methods to guarantee stability of the induction motor using the reduced-order current-fed model of the motor, i.e., by considering a third-order system with states the rotor fluxes and the motor speed, while the stator currents are the control inputs [18]–[21]. Adding to the model analysis the stator current dynamics, asymptotic stability has been proven only under the use of parameter or load torque estimators or adaptation mechanisms [22]–[29]. This means that additional dynamic designs are needed, while when the induction motor should operate with minimum losses, it becomes a cumbersome task to conduct a similar stability analysis, since the controller operation is far from the conventional FOC design. Furthermore, in all the existing literature, the converter dynamics, though crucial for the system stability, are fully omitted, often because of their nonlinear structure which increases the difficulty [30]–[32]. It is therefore obvious that a complete system modeling is required that takes into account the nonlinear structure of both the VSC and the induction motor. Moreover, on this complete model, simple control designs without additional dynamic parts that cannot be easily implemented have to be developed, while their dynamic performance should certainly ensure system stability under operation with constant or varying flux magnitude. In this frame, some early results have been proposed by the authors in [33] for a standard FOC approach.

In this study, a complete VSC-fed induction motor drive is considered. Using advanced nonlinear Hamiltonian modeling and average analysis [17], [31], [33], the complete nonlinear dynamic model of the system is obtained in a seventh-order state-space nonlinear form that includes both the ac motor and the VSC dynamics in the synchronously rotating *d-q* reference frame [32], [33]. The controlled inputs are directly the VSC

Manuscript received May 16, 2014; revised November 4, 2014; accepted December 27, 2014. This work was partially supported by the Engineering and Physical Sciences Research Council, U.K., under Grant EP/J01558X/1. Paper TEC-00342-2014.R1.

A. T. Alexandridis is with the Department of Electrical and Computer Engineering, University of Patras, Patras 26500, Greece (e-mail: a.t.alexandridis@ece.upatras.gr).

G. C. Konstantopoulos is with the Department of Automatic Control and Systems Engineering, University of Sheffield, Sheffield, S1 3JD, U.K. (e-mail: g.konstantopoulos@sheffield.ac.uk).

Q.-C. Zhong is with the Department of Automatic Control and Systems Engineering, University of Sheffield, Sheffield, S1 3JD, U.K., and also with the Department of Electrical and Computer Engineering, Illinois Institute of Technology, Chicago, IL 60616 USA (e-mail: zhongqc@ieee.org).

Color versions of one or more of the figures in this paper are available online at http://ieeexplore.ieee.org.

Digital Object Identifier 10.1109/TEC.2015.2392256

duty-ratio *d-q* components while the supplied voltage and the load torque are considered as external inputs with the second one considered to be completely unknown with step-varying magnitude. Adopting the analysis presented in [17, Sec. 10.3.8], it is first concluded that in order to achieve minimum copper losses, the square of the rotor flux magnitude should be linearly dependent from the electric torque. Extending the method under FOC steady-state operation, it is proven that the *d-q* duty-ratio input components can be used for the speed regulation through the q current tracking, while the motor efficiency takes its maximum value by regulating the d current component in a constant ratio with respect to the q current component. However, since in this case, the classical vector control analysis cannot guarantee stability with the application of simple Proportional-Integral (PI) controllers [1], [2], [22], [23], the main contribution of the present work is that the proposed system modeling permits the design of new simple nonlinear dynamic controllers, capable of overcoming these drawbacks. As proven in the present paper, the closed-loop system is stable and converges to the desired equilibrium with the rotor flux magnitude following the load variations in a manner that ensures minimum losses and field orientation at steady state. It is remarkable that an intermediate result from the adopted minimum losses analysis is that of constant slip frequency requirement under various load conditions. It is also significant to note that in this case, as it is shown in the paper, stability is achieved without needing any flux magnitude and angle estimation while the controller parameters are fully independent from the system parameters and all the other state variables except than the controlled ones; this substantially leads to simple control designs, easily and directly implemented on the *d-q* duty-ratio components although their dynamics are nonlinear. The overall design can also guarantee that the control signals, namely the duty-ratio signals, are inherently bounded in the predefined range where the converter operates with linear modulation. An industrial size 22.4-kW induction motor fed by a VSC is used to illustrate the proposed approach while comparisons with the traditional FOC technique verify the proposed minimum losses operation. Simulation results obtained with MATLAB/Simulink or a lab real-time OPAL RT system development, are provided to verify the proposed approach.

The paper is organized as follows. In Section II, the complete system model consisting of the nonlinear converter dynamics and the *d-q* dynamics of the induction motor is obtained, while the existing FOC is briefly presented. In Section III, an investigation of the system operating with minimum losses is provided, and the nonlinear controller is proposed to achieve this goal. In the sequel, closed-loop system stability analysis is proven for the complete system for the first time in the literature. Several results comparing the proposed control scheme with minimum losses over the same controller with standard FOC are presented in Section IV, while finally in Section V, some conclusions are drawn.

II. VSC Converter and Induction Motor Analysis

A. Complete Dynamic Model

The system under consideration consists of a diode rectifier, a dc-link, and a three-phase VSC feeding a three-phase induction motor, as shown in Fig. 1. A dc-link capacitor C and a smoothing inductor L are used in the dc-link along with their parasitic resistances R_C and R_L, respectively.

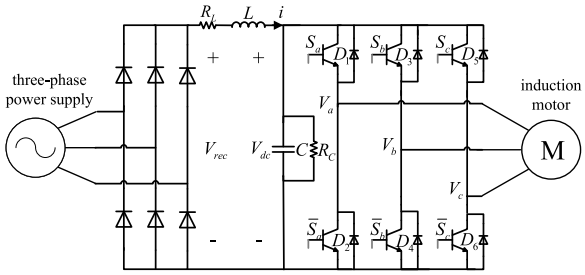

Fig. 1. Schematic diagram of the system under consideration.

Using the synchronously rotating *d-q* reference frame [1] and assuming as state variables of the induction motor the stator currents i_{ds}, i_{qs}, the rotor fluxes λ_{dr}, λ_{qr}, and the motor speed ω_r, the widely used dynamic model of the induction motor can be obtained as

$$\begin{aligned}
\sigma\dot{i}_{ds} =& -\left(\frac{R_r L_m^2}{L_r^2}+R_s\right) i_{ds} + \sigma\omega_s i_{qs} + \frac{R_r L_m}{L_r^2}\lambda_{dr} \\
&+ \frac{L_m}{L_r} p\lambda_{qr}\omega_r + V_{ds} \\
\sigma\dot{i}_{qs} =& -\left(\frac{R_r L_m^2}{L_r^2}+R_s\right) i_{qs} - \sigma\omega_s i_{qs} + \frac{R_r L_m}{L_r^2}\lambda_{qr} \\
&- \frac{L_m}{L_r} p\lambda_{dr}\omega_r + V_{qs} \\
\dot{\lambda}_{dr} =& \frac{R_r L_m}{L_r} i_{ds} - \frac{R_r}{L_r}\lambda_{dr} + (\omega_s - p\omega_r)\,\lambda_{qr} \\
\dot{\lambda}_{qr} =& \frac{R_r L_m}{L_r} i_{qs} - \frac{R_r}{L_r}\lambda_{qr} - (\omega_s - p\omega_r)\,\lambda_{dr} \\
J_m\dot{\omega}_r =& -\frac{3L_m}{2L_r} p\lambda_{qr} i_{ds} + \frac{3L_m}{2L_r} p\lambda_{dr} i_{qs} - b\omega_r - T_L
\end{aligned} \tag{1}$$

where R_s and R_r are the stator and rotor resistances, respectively, L_s and L_r are the stator and rotor inductances respectively, L_m is the mutual inductance, ω_s is the synchronous speed (reference frame), p is the number of pole pairs, J_m is the total motor and load inertia, b is the friction coefficient, T_L is the load torque, and $\sigma = L_s - \frac{L_m^2}{L_r}$. The d- and q-axis components of the stator voltages are denoted as V_{ds} and V_{qs}, respectively.

Using again the *d-q* transformation, the dynamic equations of the VSC with the dc-link can be written in the form

$$\begin{aligned}
L\dot{i} =& -R_L i - V_{dc} + V_{\rm rec} \\
C\dot{V}_{dc} =& -\frac{3}{4} m_{ds} i_{ds} - \frac{3}{4} m_{qs} i_{qs} - \frac{1}{R_C} V_{dc} + i
\end{aligned} \tag{2}$$

where i and V_{dc} are the dc-link current and voltage, respectively, and $V_{\rm rec}$ is the output voltage of the diode rectifier (almost constant). m_{ds} and m_{qs} are the d- and q-axis components of the duty-ratio signals of the VSC and are given as $m_{ds} = \frac{2V_{ds}}{V_{dc}}$ and

$m_{qs} = \frac{2V_{qs}}{V_{dc}}$ for which it holds true that [1]

$$m_a = \sqrt{m_{ds}^2 + m_{qs}^2} \tag{3}$$

with m_a being the switching duty ratio of phase-a of the induction motor voltage in a period under pulse width modulation (PWM) regulation (modulation index) and $\Delta\phi$ is the initial phase of the induction motor phase-a voltage

$$\Delta\phi = \arctan\left(\frac{m_{qs}}{m_{ds}}\right). \tag{4}$$

As a result, by combining the motor dynamics (1) with the converter dynamics (2) and taking into account the duty ratio m_{ds} and m_{qs} definitions, the complete system takes the following nonlinear matrix form:

$$M\dot{x} = \left(J\left(x, m_{ds}, m_{qs}\right) - R\right)x + G\epsilon \tag{5}$$

with the system matrices given in (6) at the bottom of the page where the state vector is $x = \left[\, i_{ds} \;\; i_{qs} \;\; \lambda_{dr} \;\; \lambda_{qr} \;\; \omega_r \;\; i \;\; V_{dc} \,\right]^T$ and the external uncontrolled input vector is $\epsilon = \left[\, -\frac{2}{3}T_L \;\; \frac{2}{3}V_{\rm rec} \,\right]^T$ which consists of bounded constant or piecewise constant signals. The only control input signals are the duty-ratio components of the VSC, i.e., m_{ds} and m_{qs}, which appear in nonlinear terms of J.

In the majority of control applications, it is preferred that the inverter operates in the "linear modulation" area [34] in order to avoid the existence of higher harmonics. This means that

$$m_a \leq 1.$$

Therefore, taking into account (3), it should be [1]

$$m_{ds}^2 + m_{qs}^2 \leq 1. \tag{7}$$

Furthermore, since the synchronous speed ω_s is produced from the inverter, it can be also specified by the control operator [1] accordingly to the desired slip frequency ω_{sl}

$$\omega_s = p\omega_r + \omega_{sl} \tag{8}$$

It should be noted that in (5), matrix M is positive definite, J is skew-symmetric, and R is positive definite. Using the storage function $H\left(x\right) = \frac{1}{2}x^T Mx$, it can be easily proven that system (5) is equivalent to the generalized Hamiltonian-passive form as determined in [31].

B. Traditional FOC Strategy

FOC technique relies on operating the induction motor as a separately excited dc motor. In most applications, the indirect rotor field orientation is applied where the total rotor flux λ_r is

$$M = \text{ diag}\left\{\sigma, \sigma, \frac{1}{L_r}, \frac{1}{L_r}, \frac{2J_m}{3}, \frac{2L}{3}, \frac{2C}{3}\right\}$$

$$J = \begin{bmatrix} 0 & \sigma\omega_s & 0 & 0 & \frac{L_m}{L_r}p\lambda_{qr} & 0 & \frac{1}{2}m_{ds} \\ -\sigma\omega_s & 0 & 0 & 0 & -\frac{L_m}{L_r}p\lambda_{dr} & 0 & \frac{1}{2}m_{qs} \\ 0 & 0 & 0 & \frac{\omega_s - p\omega_r}{L_r} & 0 & 0 & 0 \\ 0 & 0 & -\frac{\omega_s - p\omega_r}{L_r} & 0 & 0 & 0 & 0 \\ -\frac{L_m}{L_r}p\lambda_{qr} & \frac{L_m}{L_r}p\lambda_{dr} & 0 & 0 & 0 & 0 & 0 \\ 0 & 0 & 0 & 0 & 0 & 0 & -\frac{2}{3} \\ -\frac{1}{2}m_{ds} & -\frac{1}{2}m_{qs} & 0 & 0 & 0 & \frac{2}{3} & 0 \end{bmatrix}$$

$$G = \begin{bmatrix} 0 & 0 & 0 & 0 & 1 & 0 & 0 \\ 0 & 0 & 0 & 0 & 0 & 1 & 0 \end{bmatrix}^T \text{ and}$$

$$R = \begin{bmatrix} \frac{R_r L_m^2}{L_r^2} + R_s & 0 & -\frac{R_r L_m}{L_r^2} & 0 & 0 & 0 & 0 \\ 0 & \frac{R_r L_m^2}{L_r^2} + R_s & 0 & -\frac{R_r L_m}{L_r^2} & 0 & 0 & 0 \\ -\frac{R_r L_m}{L_r^2} & 0 & \frac{R_r}{L_r^2} & 0 & 0 & 0 & 0 \\ 0 & -\frac{R_r L_m}{L_r^2} & 0 & \frac{R_r}{L_r^2} & 0 & 0 & 0 \\ 0 & 0 & 0 & 0 & \frac{2}{3}b & 0 & 0 \\ 0 & 0 & 0 & 0 & 0 & \frac{2}{3}R_L & 0 \\ 0 & 0 & 0 & 0 & 0 & 0 & \frac{2}{3R_C} \end{bmatrix} \tag{6}$$

aligned on the synchronous rotating d-axis, i.e.

$$\lambda_r = \lambda_{dr} \quad \text{and} \quad \lambda_{qr} = 0. \tag{9}$$

In this frame, the rotor flux dynamics can be decoupled and lead to a simplified control scheme. Assuming steady-state operation, one can determine the desired slip frequency from the fourth equation of (5) as

$$\omega_s - p\omega_r \equiv \omega_{sl} = \frac{L_m}{\tau_r \lambda_r} i_{qs} \tag{10}$$

where $\tau_r = \frac{L_r}{R_r}$ is the rotor time constant. Since the rotor flux cannot be measured, the amplitude of the flux is usually estimated from the third equation of system (5) as

$$\tau_r \dot{\hat{\lambda}}_r + \hat{\lambda}_r = L_m i_{ds} \tag{11}$$

where $\hat{\lambda}_r$ is the estimation of the total rotor flux [22].

In order to achieve fast dynamics below the rated speed, the rotor flux is usually maintained constant, and therefore, the reference signals are the desired motor speed ω_r^{ref} and the rotor flux $\hat{\lambda}_r$. Assuming steady-state operation, $\hat{\lambda}_r = \bar{\lambda}_r$, one can define from (11) the d-axis current $\bar{i}_{ds}$ as follows:

$$\bar{\lambda}_r = L_m \bar{i}_{ds}. \tag{12}$$

Therefore, traditional FOC techniques provide a constant reference value for the flux which can be transformed into a constant reference for the current $\bar{i}_{ds} = i_{ds}^{\text{ref}}$. Traditional PI and cascaded PI controllers as well as nonlinear controllers, as those proposed by the authors in [33], can be used to achieve the desired regulation.

However, in many cases where power losses play a key role in the system operation, a modified control strategy that also achieves this task is required [17]. In the following section, using a suitable nonlinear controller, the work of [33] is extended to achieve minimum losses and field orientation at steady state with guaranteed nonlinear closed-loop system stability and convergence to the desired equilibrium.

III. Nonlinear Controller for Achieving Minimum Losses

A. Operation with Minimum Losses

A lot of research has been conducted in the literature for operating the induction machine with minimum losses [10]–[16]. Induction motor losses are given from the following expression:

$$\begin{aligned} P_{\text{loss}} &= P_{\text{supplied}} - P_{\text{mech}} \\ &\approx \frac{3}{2}(V_{ds} i_{ds} + V_{qs} i_{qs}) - T_e \omega_r \end{aligned} \tag{13}$$

where T_e is the electromagnetic torque. Taking into account the induction motor model (1), it can be easily shown that P_{loss} minimization requires an optimal rotor flux λ_r^{opt} as given by the following expression [17, Sec. 10.3.8]:

$$\left(\lambda_r^{\text{opt}}\right)^2 = \sqrt{\frac{L_r^2}{p^2} + \frac{R_r L_m^2}{R_s p^2}}\, |T_d| \tag{14}$$

where here it is considered at steady state that $|T_d| = \frac{2}{3}|T_e|$, which implies that the square of the rotor flux magnitude should be linearly dependent from the electromagnetic torque.

In this paper, the main tasks are to achieve accurate speed regulation with both field orientation and losses minimization at steady state. Assuming FOC operation at steady state where the stator currents are denoted by $\bar{i}_{ds}$ and $\bar{i}_{qs}$, the electromagnetic torque is given as

$$T_e = \frac{3}{2} p \frac{L_m^2}{L_r} \bar{i}_{ds} \bar{i}_{qs} \tag{15}$$

where now the optimal flux as given by (12) is not locked on a constant value. Therefore, considering a varying flux magnitude

$$\lambda_r^{\text{opt}} = L_m \bar{i}_{ds} \tag{16}$$

with $\bar{i}_{ds}$ appropriately varying to satisfy (14) and substituting (15) and (16) into (14) one arrives at

$$L_m^2 \bar{i}_{ds}^2 = \sqrt{\frac{L_r^2}{p^2} + \frac{R_r L_m^2}{R_s p^2}}\, p \frac{L_m^2}{L_r} \bar{i}_{ds} \bar{i}_{qs}.$$

Defining the stator d-q currents ratio as $l^{\text{opt}} = \frac{\bar{i}_{qs}}{\bar{i}_{ds}}$, one can easily obtain

$$l^{\text{opt}} = \frac{\bar{i}_{qs}}{\bar{i}_{ds}} = \frac{1}{\sqrt{1 + \frac{R_r L_m^2}{R_s L_r^2}}}. \tag{17}$$

At this point, it is noted that recalling FOC theory of Section II-B, by substituting (12) into (10), the steady-state slip frequency that leads to optimal operation with minimum losses has to be constant as the following expression indicates:

$$\omega_{sl}^{\text{opt}} = \frac{1}{\tau_r} \frac{\bar{i}_{qs}}{\bar{i}_{ds}} = \frac{l^{\text{opt}}}{\tau_r} = \text{const.} \tag{18}$$

As a result, if the stator currents are controlled in accordance to (17), then operation with globally minimum losses is achieved as long as the resulting flux magnitude is below its upper allowable bound. In practical applications, however, the calculated l^{opt} value is too small, resulting in unacceptable high flux magnitudes; then, the meaning of (17) is to select the smallest possible value for the l^{opt} (bigger than the one calculated from (17)) which can ensure operation with locally minimum losses and flux magnitude strengthened close to its upper bound.

Under these circumstances, stability analysis should be always guaranteed not only at steady state but during the transient performance as well. Such an analysis based on a controller that achieves all the previous tasks and which provides accurate speed regulation is given in the following section.

B. Nonlinear Controller Design and Analysis

Since the complete dynamic system (5) is nonlinear, in order to obtain closed-loop stability, a nonlinear controller is required. The proposed controller presented in this section, which is applied at the control inputs m_{ds} and m_{qs} of the converter, is proven to achieve precise motor speed regulation at ω_r^{ref} and minimum losses in a field-oriented operation, as discussed in

the previous section. The control structure is given as

$$m_{ds} = z_1 \tag{19}$$

$$m_{qs} = z_2 \tag{20}$$

where

$$\dot{z} = A_{\text{contr}}\left(z, \omega_r, i_{ds}, i_{qs}\right) z \tag{21}$$

with A_{contr}

$$= \begin{bmatrix} 0 & 0 & -k_1\left(i_{ds} - \dfrac{i_{qs}}{l^{\text{opt}}}\right) \\ 0 & 0 & -k_2\left(\omega_r - \omega_r^{\text{ref}}\right) \\ k_1\left(i_{ds} - \dfrac{i_{qs}}{l^{\text{opt}}}\right) & k_2\left(\omega_r - \omega_r^{\text{ref}}\right) & -c\left(z_1^2 + z_2^2 + z_3^2 - 1\right) \end{bmatrix}.$$

States $z = \begin{bmatrix} z_1 & z_2 & z_3 \end{bmatrix}^T$ represent the controller dynamics, k_1, k_2 are two nonzero constant gains, and c is positive constant. It becomes clear from the controller dynamics (21) that if ω_r is regulated at ω_r^{ref} and the ratio of i_{qs} and i_{ds} is maintained constant and equal to l^{opt} at steady state, then the controller states will converge to three equilibrium constant values z_1^*, z_2^*, z_3^*.

It can be easily seen that the proposed controller (21) implies that the control law acts as an attractive limit cycle for the controller states z_1, z_2, z_3 on the surface of a sphere C_r with center the origin and radius equal to 1, i.e.

$$C_r = \left\{z_1, z_2, z_3 : z_1^2 + z_2^2 + z_3^2 = 1\right\}.$$

As it is obvious, by introducing the term $-c\left(z_1^2 + z_2^2 + z_3^2 - 1\right)$ in (21), the controller states are attracted and remain all time thereafter on sphere C_r. This means that the z_1, z_2, z_3 trajectories rove over till reach an equilibrium z_1^*, z_2^*, z_3^* as ω_r and i_{ds} approach their reference values, while the robustness of z_1, z_2, z_3 crucially increases in the sense that, if for any reason z_1^*, z_2^*, z_3^* are disturbed, they cannot leave C_r. Since the controller states are restricted on the surface of sphere C_r, then obviously each state is bounded in the set $[-1, 1]$ and as a result

$$\left(z_1\left(t\right)\right)^2 + \left(z_2\left(t\right)\right)^2 = 1 - \left(z_3\left(t\right)\right)^2$$

$$\text{or } \left(z_1\left(t\right)\right)^2 + \left(z_2\left(t\right)\right)^2 \leq 1$$

which implies that (7) is obviously satisfied. Therefore, the proposed controller can guarantee that the VSC will always operate in the linear modulation area where $0 \leq m_a \leq 1$, i.e., the technical limits of the duty-ratio input are fulfilled. For further details about the general concept of the controller operation, the reader is referred to [33], though the controller dynamics in the present paper are quite different from those presented in [33], as imposed by the different controller tasks.

C. Closed-Loop System Modeling and Stability Analysis

After incorporating the controller dynamics (21) to the complete VSC-motor system (5), the resulting closed-loop system is still given in the generalized nonlinear Hamiltonian-passive form

$$\tilde{M}\dot{\tilde{x}} = \left(\tilde{J}\left(\tilde{x}\right) - \tilde{R}\right)\tilde{x} + \tilde{G}\epsilon \tag{22}$$

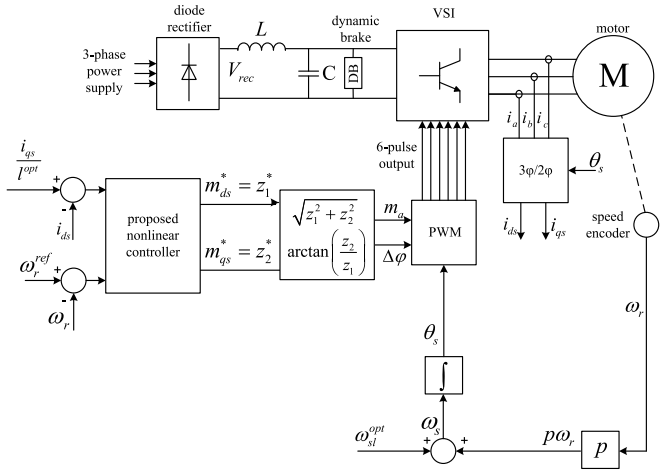

Fig. 2. Nonlinear controller for achieving speed regulation with minimum losses.

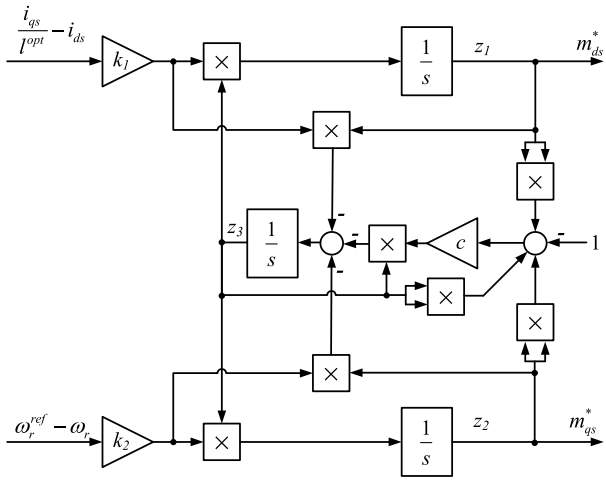

Fig. 3. Proposed nonlinear controller implementation.

where the closed-loop system is of tenth order with matrices

$$\tilde{M} = \begin{bmatrix} M & 0_{7\times3} \\ 0_{3\times7} & I_3 \end{bmatrix},\ \tilde{G} = \begin{bmatrix} G^T & 0_{2\times3} \end{bmatrix}^T$$

$$\tilde{R} = \begin{bmatrix} R & 0_{7\times3} \\ 0_{3\times7} & R_{cl} \end{bmatrix}, \text{ with } R_{cl} = \begin{bmatrix} 0_{2\times2} & 0_{2\times1} \\ 0_{1\times2} & -c\left(z_1^2 + z_2^2 + z_3^2 - 1\right) \end{bmatrix}$$

and $\tilde{J}$ as given in Appendix. The closed-loop state vector is $\tilde{x} = \begin{bmatrix} x^T & z^T \end{bmatrix}^T = \begin{bmatrix} i_{ds} & i_{qs} & \lambda_{dr} & \lambda_{qr} & \omega_r & i & V_{dc} & z_1 & z_2 & z_3 \end{bmatrix}^T$.

One can easily see that matrix $\tilde{M}$ remains symmetric and positive definite, $\tilde{J}$ is still skew-symmetric, and $\tilde{R}$ matrix is symmetric. Also, the system dynamics remain in its full form without any simplification caused by the field-oriented demand. The schematic diagram of the proposed nonlinear controller applied on the complete system is given in Fig. 2, while the controller implementation is depicted in Fig. 3.

To begin with the stability analysis, consider first the unforced closed-loop system ($\epsilon = 0$)

$$\tilde{M}\dot{\tilde{x}} = \left(\tilde{J}\left(\tilde{x}\right) - \tilde{R}\right)\tilde{x} \tag{23}$$

with storage function candidate

$$V\left(\tilde{x}\right) = \frac{1}{2}x^T Mx + \frac{1}{4}\left(z_1^2 + z_2^2 + z_3^2 - 1\right)^2. \tag{24}$$

Then, the time derivative of V is calculated as

$$\begin{aligned}\dot{V} = & \; x^T M\dot{x} + \frac{1}{2}\left(z_1^2 + z_2^2 + z_3^2 - 1\right) \\ & \left(2z_1\dot{z}_1 + 2z_2\dot{z}_2 + 2z_3\dot{z}_3\right) \\ = & \; -x^T Rx - c\left(z_1^2 + z_2^2 + z_3^2 - 1\right)^2 z_3^2 \leq 0\end{aligned} \tag{25}$$

which proves the stability of system (23) as follows. System (23) is a nonlinear autonomous system and since the storage function (24) is radially unbounded with nonpositive derivative over the whole state space, then according to the Global Invariant Set Theorem 3.5 described in [35], all solutions uniformly globally asymptotically converge to the largest invariant set N in E. Set E is defined as the set where $\dot{V} = 0$ and since $R > 0$, then it consists of the union of $x = 0$ and z_1, z_2, z_3 constrained on sphere C_r.

Furthermore, from the matrix-diagonal form of matrices $\tilde{M}$, $\tilde{J}$, and $\tilde{R}$, it becomes clear that the induction motor-converter system (plant) and the controller system can be handled separately in both the closed-loop unforced system (23) and the original one, as given by (22). Particularly, as shown in the previous analysis, the controller system operates as an attractive sphere for the states z_1, z_2, and z_3, independently from the controlled plant states i_{ds}, i_{qs}, ω_r, and the external input ϵ. Thus, exploiting this significant controller property to the closed-loop system analysis, the controller state vector z is considered as a bounded time-varying vector for the plant system

$$M\dot{x} = \left(J\left(x, z(t)\right) - R\right)x + G\epsilon \tag{26}$$

which is handled independently as a nonautonomous nonlinear system with external input vector ϵ.

For system (26) consider the Lyapunov function candidate

$$W = \frac{1}{2}x^T Mx. \tag{27}$$

Taking the time derivative of W, it yields

$$\dot{W} = -x^T Rx + x^T G\epsilon. \tag{28}$$

Then, it can be easily shown [36] that there exist $0 < \theta < 1$ such that

$$\dot{W} \leq -(1-\theta)\lambda_{\min}(R)\left\|x\right\|^2 \; \forall \left\|x\right\| \geq \frac{\left\|\epsilon\right\|}{\theta\lambda_{\min}(R)} \tag{29}$$

where $\lambda_{\min}(R)$ is the smallest eigenvalue of the constant positive definite matrix R and, in this case, $\|G\epsilon\| = \|\epsilon\|$. Inequality (29) proves that system (26) is input-to-state stable with respect to the external input ϵ [37], [36]. Therefore, since the external input vector ϵ is a bounded signal consisting of the diode rectifier voltage and the load torque, then the converter-motor system is stable in the sense of boundedness, i.e., x is bounded. Furthermore, since z_1, z_2, and z_3 are attracted on a closed set described by sphere C_r, then it is concluded that the whole closed-loop state vector $\tilde{x}$ is bounded.

Assuming that the reference signals and the external input vector ϵ are provided in a manner that technically result in an equilibrium point (certainly within the converter-motor system requirements), then for the closed-loop system which is given in the Hamiltonian-passive form [31] and under some common assumptions mentioned in [31], it is proven that the bounded states $\tilde{x}$ will eventually converge to the desired equilibrium.

TABLE I
SYSTEM PARAMETERS

motor rated power P_n	22.4 kW
rated stator voltage V_s	230 V
rated stator current I_s	39.5 A
rated speed ω_m	1168 r/min
diode rectifier output $V_{\rm rec}$	670 V
dc-link capacitance C	1.8 mF
dc-link inductance L	3 mH
dc-link resistance R_L	0.05 Ω
stator inductance L_s	44.2 mH
rotor inductance L_r	41.7 mH
mutual inductance L_m	41 mH
stator resistance R_s	0.294 Ω
rotor resistance R_r	0.156 Ω
pole pairs p	3
motor-load inertia J_m	0.4 kg · m^2
friction coefficient b	0.003 N · m · s/rad

IV. RESULTS

A. Validation with MATLAB/Simulink Results

In order to evaluate the proposed controller performance, an industrial size 22.4-kW induction motor fed by a VSC is considered. The proposed controller is used to achieve minimum losses and is compared to the controller with FOC as described in [33] for the same speed regulation scenario. The system parameters are analytically presented in Table I.

Starting from a motor speed equal to 80 rad/s, at the time instant $t = 3$ s the reference speed is set to $\omega_r^{\rm ref} = 110$ rad/s, at $t = 6$ s it drops to 90 rad/s and at $t = 9$ s it changes again to 100 rad/s. At time instant $t = 12$ s and while the reference speed is maintained at $\omega_r^{\rm ref} = 100$ rad/s, the load torque T_L drops by 7% and 3 s later, it increases rapidly by 15%. These scenario is performed to check the performance under several reference and load changes. In all cases, the parameters of both nonlinear controllers are $k_1 = -1\,A^{-1}$, $k_2 = 0.05$ s/rad, and $c = 1000$. From (17), the calculated value $l^{\rm opt} = 0.813$ is too small, resulting in flux magnitude bigger than its upper allowable bound of 1 Wb and, therefore, following the analysis described in Section III-A, $l^{\rm opt} = 1.85$ is used.

Fig. 4 shows the time response of the complete converter-motor system states and input. The responses of the stator currents are provided in Fig. 4(a) and (b), where it is clear that the controller with FOC regulates the d-axis current to the desired value $i_{ds}^{\rm ref} = 19\,A$, as described in Section II-B. On the other

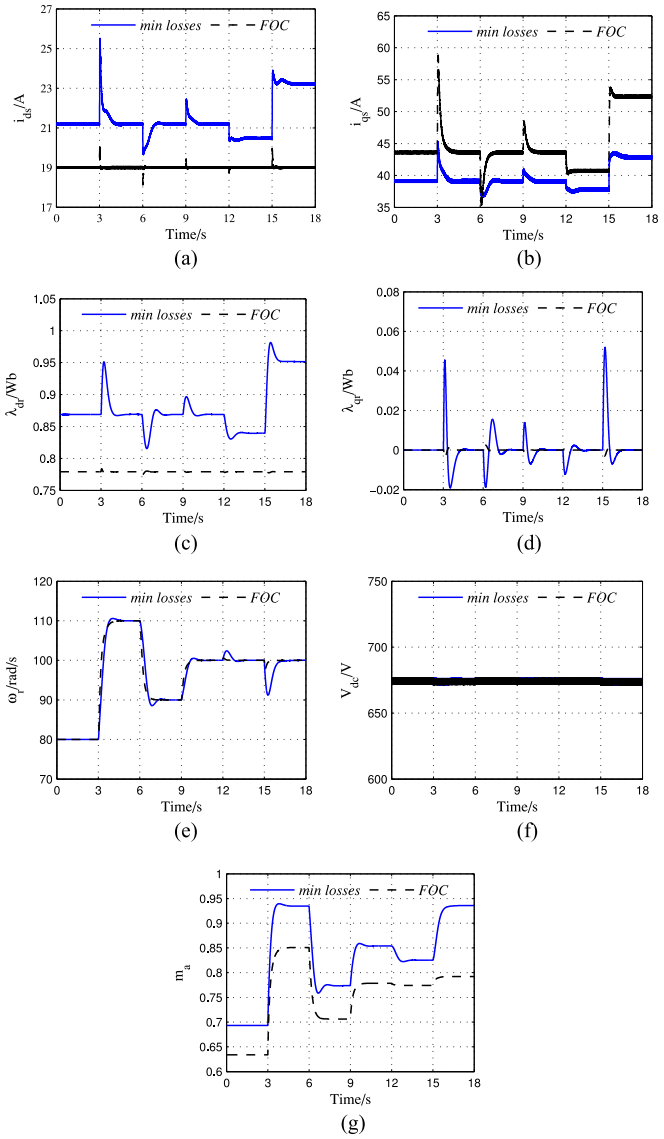

Fig. 4. Complete system response for the proposed nonlinear controller with minimum losses and the nonlinear controller with standard FOC. (a) *d*-axis stator current. (b) *q*-axis stator current. (c) *d*-axis rotor flux. (d) *q*-axis rotor flux. (e) Motor speed. (f) DC-link capacitor voltage. (g) Modulation index.

hand, the nonlinear controller with minimum losses regulates i_{ds} and i_{qs} in such values in order to have a constant ratio equal to $l^{\rm opt}$ at steady state. From the rotor flux responses in Fig. 4(c) and (d), it is clear that both controllers achieve field orientation at steady state since $\lambda_{qr} = 0$. Additionally, it is observed that the proposed controller provides operation with locally minimum losses and flux magnitude strengthened below its upper bound (Fig. 4(c)). Both controllers achieve precise motor speed regulation for every reference change and load disturbances as shown in Fig. 4(e). However, the controller with minimum losses provides a slightly slower response but this is the cost for minimizing the losses at steady state. The dc-link voltage $V_{\rm dc}$, shown in Fig. 4(f), is regulated according to the system equilibrium where the fluctuations are caused from the fact that the output voltage $V_{\rm rec}$ of the diode rectifier is not strictly constant. Finally, in Fig. 4(g), it is verified that the proposed controller

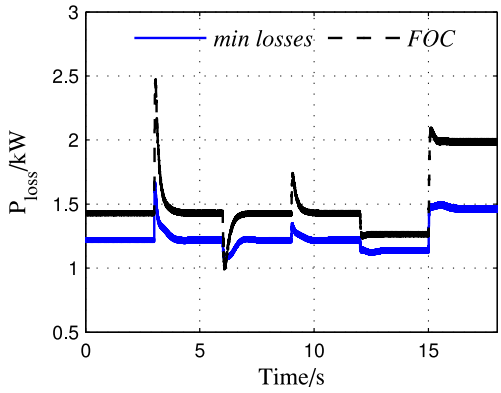

Fig. 5. Power losses using the nonlinear controller with minimum losses and the nonlinear controller with standard FOC.

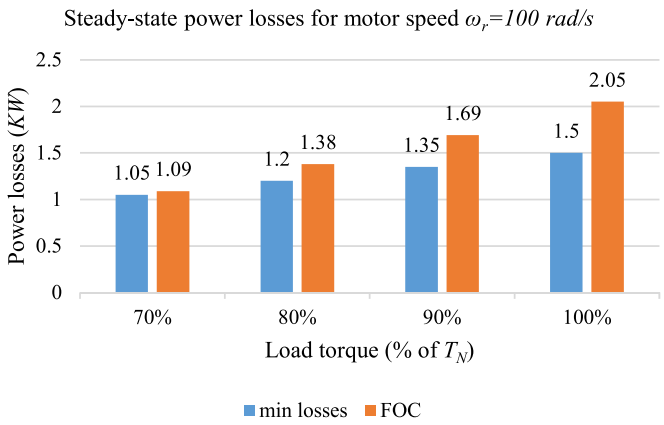

Fig. 6. Steady-state power losses for different load torque values and for constant motor speed $\omega_r = 100$ rad/s using the nonlinear controller with minimum losses and the nonlinear controller with standard FOC.

forces the duty-ratio signals to remain bounded and operate the VSC in the linear PWM mode, as analytically presented in this paper.

In order to check the main task of the proposed controller, the system power losses are calculated and presented in Fig. 5 for the whole scenario. It can be easily verified that the proposed controller significantly reduces the power losses with respect to the traditional FOC techniques. Especially after the final load torque increase, the power losses are reduced by 25%. The steady-state losses for a given motor speed $\omega_r = 100$ rad/s and for several load torque values T_L (in percentage over the rated torque T_N) are summarized in Fig. 6, where it is observed the significant reduction of motor losses using the proposed approach compared to the traditional FOC technique. Therefore, the same speed regulation can be achieved with slightly sacrificing the transient performance, but the steady-state losses will be significantly reduced by the technique proposed in the present paper.

B. Validation with Real-Time Results

To further validate the proposed control approach, real-time results have been obtained using the real-time system of OPAL-RT for a converter-induction motor system with similar

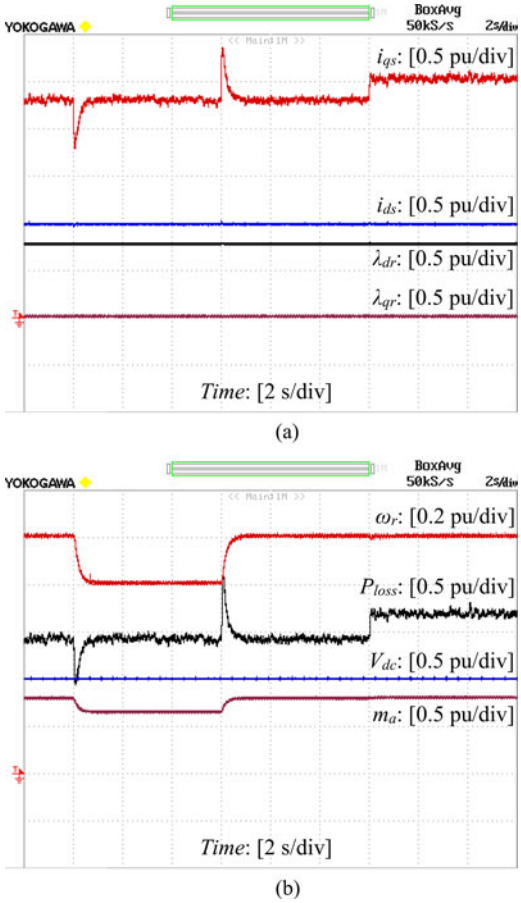

Fig. 7. Real-time results for the nonlinear controller with standard FOC. (a) d, q-axis stator currents and rotor fluxes. (b) Motor speed, power losses, DC-link capacitor voltage and modulation index.

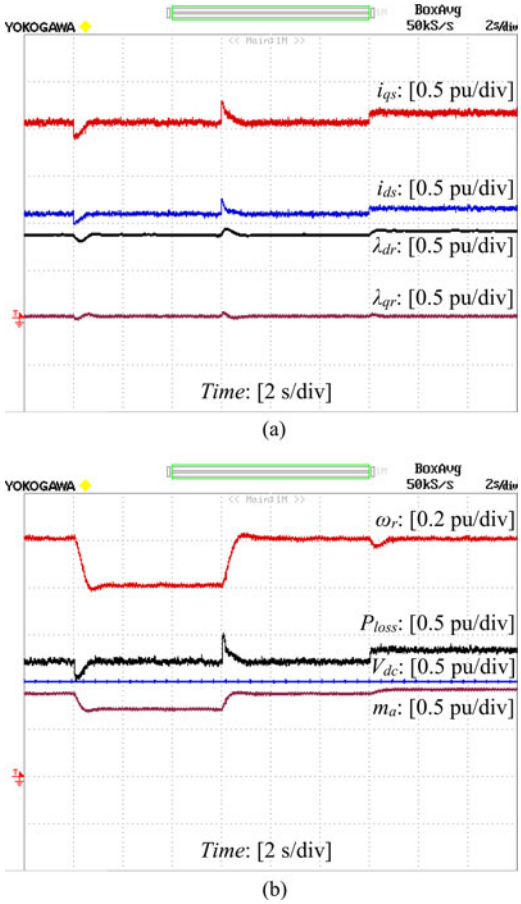

Fig. 8. Real-time results for the nonlinear controller with minimum losses. (a) d, q-axis stator currents and rotor fluxes. (b) Motor speed, power losses, DC-link capacitor voltage and modulation index.

parameters (in pu). Once again, both the proposed controller for minimum losses and the controller with FOC are compared. In this scenario, the reference motor speed is initially set to $\omega_r^{\rm ref} = 1\,$p.u., at time instant $t = 2\,$s it drops to $\omega_r^{\rm ref} = 0.8\,$p.u. and at $t = 8\,$s it is set back to 1 p.u. Finally, at $t = 14\,$s, a 15% increase is applied at the load torque. Note that for the controller with FOC, the reference d-axis current is set at $i_{ds}^{\rm ref} = 1\,$p.u. during the whole operation.

The results for the nonlinear controller with standard FOC are shown in Fig. 7, while the same scenario with the proposed controller operating with minimum losses is shown in Fig. 8. As it is shown in Fig. 7(a), the controller with FOC regulates the d-axis current at the desired value and achieves field orientation at all times since λ_{qr} is regulated at zero. The rest of the controller states are regulated at their steady-state values with very small transients. Additionally, the controller suitably regulates the motor speed at its desired value under the reference change and under the sudden load change, as shown in Fig. 7(b). The dc-bus voltage stays always constant at 1 p.u., the modulation index remains below 1 at all times, and the response of the losses ($P_{\rm loss}$) is observed in the same figure. On the other hand, the results for the proposed controller operating with minimum losses are shown in Fig. 8. Field orientation is also achieved at steady state since the q-axis rotor flux is regulated at zero, i.e., $\lambda_{qr} = 0$ at steady state and the stator currents are controlled to have a constant ratio $l^{\rm opt} = \frac{i_{qs}}{i_{ds}}$ at steady state, as shown in Fig. 8(a). However, a slightly larger transient is observed compared to the controller with the standard FOC. As it is verified in Fig. 8(b), the motor speed is regulated at its reference value after the reference and the load changes, the dc-bus voltage is constant at 1 p.u., and once again the modulation index stays below 1, as imposed by the controller operation. From Fig. 8(b), it is fully verified in agreement with the theoretical analysis, that the proposed method achieves significant reduction of the machine losses $P_{\rm loss}$, during the whole operation (steady state and transient). Nevertheless, it becomes clear from the comparison of the motor speed responses, shown in Figs. 7(b) and 8(b) between the case of using the controller with the standard FOC and the case of using the controller which constrains the system to operate with minimum losses, respectively, that the cost to pay, is only a slightly larger transient; however, the simple design and the overall system performance, seems to be in favour of applying the proposed approach.

V. Conclusion

In this paper, a complete nonlinear system modeling of a VSC-fed induction motor was presented, and a nonlinear

$$\tilde{J} = \begin{bmatrix} 0 & \sigma\omega_s & 0 & 0 & \frac{L_m}{L_r}p\lambda_{qr} & 0 & \frac{1}{2}z_1 & 0_{1\times 3} \\ -\sigma\omega_s & 0 & 0 & 0 & -\frac{L_m}{L_r}p\lambda_{dr} & 0 & \frac{1}{2}z_2 & 0_{1\times 3} \\ 0 & 0 & 0 & \frac{l^{\mathrm{opt}}}{\tau_r L_r} & 0 & 0 & 0 & 0_{1\times 3} \\ 0 & 0 & -\frac{l^{\mathrm{opt}}}{\tau_r L_r} & 0 & 0 & 0 & 0 & 0_{1\times 3} \\ -\frac{L_m}{L_r}p\lambda_{qr} & \frac{L_m}{L_r}p\lambda_{dr} & 0 & 0 & 0 & 0 & 0 & 0_{1\times 3} \\ 0 & 0 & 0 & 0 & 0 & 0 & -\frac{2}{3} & 0_{1\times 3} \\ -\frac{1}{2}z_1 & -\frac{1}{2}z_2 & 0 & 0 & 0 & \frac{2}{3} & 0 & 0_{1\times 3} \\ 0_{3\times 1} & 0_{3\times 1} & 0_{3\times 1} & 0_{3\times 1} & 0_{3\times 1} & 0_{3\times 1} & 0_{3\times 1} & J_c \end{bmatrix}$$

dynamic controller was proposed to achieve precise motor speed regulation with minimum losses. Taking into account the varying rotor flux theory, the relationship between the stator currents is obtained to minimize the power losses and achieve field orientation at steady state. Both the current and speed regulation is implemented by a nonlinear controller that is fully independent from the system parameters and produces bounded duty-ratio signals always within the predefined limits as they are set by the linear modulation area of the converter. Based on the complete system dynamics and the controller structure, nonlinear closed-loop system stability is proven where the system states are guaranteed to remain bounded and converge to the desired equilibrium. Adding to the rigorous stability analysis the fact that the controller can be easily implemented with no flux measurements or estimation needed, this control scheme establishes a clearly innovated step in ac motor drives that decisively enhances the existing techniques.

APPENDIX

Appendix equation shown at the top of the page where $\omega_s = p\omega_r + \omega_{sl}^{\mathrm{opt}}$ and

$$J_c = \begin{bmatrix} 0 & 0 & -k_1\left(i_{ds} - \frac{i_{qs}}{l^{\mathrm{opt}}}\right) \\ 0 & 0 & -k_2\left(\omega_r - \omega_r^{\mathrm{ref}}\right) \\ k_1\left(i_{ds} - \frac{i_{qs}}{l^{\mathrm{opt}}}\right) & k_2\left(\omega_r - \omega_r^{\mathrm{ref}}\right) & 0 \end{bmatrix}.$$

REFERENCES

[1] B. K. Bose, *Modern Power Electronics and AC Drives*. Upper Saddle River, NJ, USA: Prentice-Hall, 2002.

[2] N. P. Quang and J.-A. Dittrich, *Vector Control of Three-Phase AC Machines: System Development in the Practice*. New York, NY, USA: Springer, 2008.

[3] G. D. Marques and D. M. Sousa, "Stator flux active damping methods for field-oriented doubly fed induction generator," *IEEE Trans. Energy Convers.*, vol. 27, no. 3, pp. 799–806, Sep. 2012.

[4] Y. Zhou, P. Bauer, J. A. Ferreira, and J. Pierik, "Operation of grid-connected DFIG under unbalanced grid voltage condition," *IEEE Trans. Energy Convers.*, vol. 24, no. 1, pp. 240–246, Mar. 2009.

[5] G. Kenne, T. Ahmed-Ali, F. Lamnabhi-Lagarrigue, and A. Arzande, "Real-time speed and flux adaptive control of induction motors using unknown time-varying rotor resistance and load torque," *IEEE Trans. Energy Convers.*, vol. 24, no. 2, pp. 375–387, Jun. 2009.

[6] A. Makouf, M. E. H. Benbouzid, D. Diallo, and N.-E. Bouguechal, "A practical scheme for induction motor speed sensorless field-oriented control," *IEEE Trans. Energy Convers.*, vol. 19, no. 1, pp. 230–231, Mar. 2004.

[7] M. K. Bourdoulis and A. T. Alexandridis, "Direct power flow modeling and simple controller design for ac/dc voltage-source converters," in *Proc. 39th Annu. Conf. IEEE Ind. Electron. Soc.,* 2013, pp. 637–642.

[8] M. K. Bourdoulis and A. T. Alexandridis, "Nonlinear stability analysis of DFIG wind generators in voltage oriented control operation," in *Proc. Eur. Control Conf.*, 2013, pp. 484–489.

[9] M. K. Bourdoulis and A. T. Alexandridis, "Rotor-side cascaded PI controller design and gain tuning for DFIG wind turbines," in *Proc. 4th Int. Conf. Power Eng. Energy Elect. Drives*, 2013, pp. 733–738.

[10] R. P. d. M. Martins, D. M. Sousa, V. F. Pires, and R. A.,, "Reducing the power losses of a commercial electric vehicle: Analysis based on an asynchronous motor control," in *Proc. 4th Int. Conf. Power Eng. Energy Elect. Drives*, 2013, pp. 1247–1252.

[11] B.-A. Chen, T.-K. Lu, C. W.-L., and Z.-C. Lee, "An analytical approach to maximum power tracking and loss minimization of a doubly fed induction generator considering core loss," *IEEE Trans. Energy Convers.*, vol. 27, no. 2, pp. 449–456, Jun. 2012.

[12] R. Leidhold, G. Garcia, and M. I. Valla, "Field-oriented controlled induction generator with loss minimization," *IEEE Trans. Ind. Electron.*, vol. 49, no. 1, pp. 147–156, Feb. 2002.

[13] Y. Lei, A. Mullane, G. Lightbody, and R. Yacamini, "Modeling of the wind turbine with a doubly fed induction generator for grid integration studies," *IEEE Trans. Energy Convers.*, vol. 21, no. 1, pp. 257–264, Mar. 2006.

[14] Z. Qu, M. Ranta, M. Hinkkanen, and J. Luomi, "Loss-minimizing flux level control of induction motor drives," *IEEE Trans. Ind. Appl.*, vol. 48, no. 3, pp. 952–961, May/Jun. 2012.

[15] C. Canudas de Wit, and J. Ramirez, "Optimal torque control for current-fed induction motors," *IEEE Trans. Autom. Control*, vol. 44, no. 5, pp. 1084–1089, May 1999.

[16] M. Waheeda Beevi, A. Sukeshkumar, and N. Nair, "New online loss-minimization-based control of scalar and vector-controlled induction motor drives," in *Proc. IEEE Int. Conf. Power Electron., Drives Energy Syst.*, 2012, pp. 1–7.

[17] R. Ortega, A. Loria, P. J. Nicklasson, and H. Sira-Ramirez, *Passivity-based Control of Euler-Lagrange Systems, Mechanical, Electrical and Electromechanical Applications*. New York, NY, USA: Springer, 1998.

[18] P. A. De Wit, R. Ortega, and I. Mareels, "Indirect field-oriented control of induction motors is robustly globally stable," *Automatica*, vol. 32, no. 10, pp. 1393–1402, 1996.

[19] W.-J. Wang and J.-Y. Chen, "Compositive adaptive position control of induction motors based on passivity theory," *IEEE Trans. Energy Convers.*, vol. 16, no. 2, pp. 180–185, Jul. 2001.

[20] G. Chang, J. P. Hespanha, A. S. Morse, M. Netto, and R. Ortega, "Supervisory field-oriented control of induction motors with uncertain rotor resistance," *Int. J. Adaptive Control Signal Process.*, vol. 15, no. 3, pp. 353–375, 2001.

[21] R. Reginatto and A. S. Bazanella, "Robustness of global asymptotic stability in indirect field-oriented control of induction motors," *IEEE Trans. Autom. Control*, vol. 48, no. 7, pp. 1218–1222, Jul. 2003.

[22] M. N. Marwali, A. Keyhani, and W. Tjanaka, "Implementation of indirect vector control on an integrated digital signal processor-based system," *IEEE Trans. Energy Convers.*, vol. 14, no. 2, pp. 139–146, Jun. 1999.
[23] H. A. Toliyat, E. Levi, and M. Raina, "A review of RFO induction motor parameter estimation techniques," *IEEE Trans. Energy Convers.*, vol. 18, no. 2, pp. 271–283, Jun. 2003.
[24] R. Ortega, P. J. Nicklasson, and G. Espinosa-Pérez, "On speed control of induction motors," *Automatica*, vol. 32, no. 3, pp. 455–460, 1996.
[25] S. Peresada, A. Tonielli, and R. Morici, "High-performance indirect field-oriented output-feedback control of induction motors," *Automatica*, vol. 35, no. 6, pp. 1033–1047, 1999.
[26] D. Karagiannis, A. Astolfi, R. Ortega, and M. Hilairet, "A nonlinear tracking controller for voltage-fed induction motors with uncertain load torque," *IEEE Trans. Control Syst. Technol.*, vol. 17, no. 3, pp. 608–619, May 2009.
[27] P. J. Nicklasson, R. Ortega, G. Espinosa-Perez, and C. Jacobi, "Passivity-based control of a class of Blondel-Park transformable electric machines," *IEEE Trans. Autom. Control*, vol. 42, no. 5, pp. 629–647, May 1997.
[28] S. Peresada and A. Tonielli, "High-performance robust speed-flux tracking controller for induction motor," *Int. J. Adaptive Control Signal Process.*, vol. 14, nos. 2/3, pp. 177–200, 2000.
[29] A. Behal, M. Feemster, and D. Dawson, "An improved indirect field-oriented controller for the induction motor," *IEEE Trans. Control Syst. Technol.*, vol. 11, no. 2, pp. 248–252, Mar. 2003.
[30] T.-S. Lee, "Lagrangian modeling and passivity-based control of three-phase AC/DC voltage-source converters," *IEEE Trans. Ind. Electron.*, vol. 51, no. 4, pp. 892–902, Aug. 2004.
[31] G. C. Konstantopoulos and A. T. Alexandridis, "Generalized nonlinear stabilizing controllers for Hamiltonian-passive systems with switching devices," *IEEE Trans. Control Syst. Technol.*, vol. 21, no. 4, pp. 1479–1488, Jul. 2013.
[32] G. C. Konstantopoulos and A. T. Alexandridis, "Design and analysis of a novel bounded nonlinear controller for three-phase ac/dc converters," in *Proc. IEEE 52nd Annu. Conf. Decision Control*, 2013, pp. 3659–3664.
[33] G. C. Konstantopoulos, A. T. Alexandridis, and E. D. Mitronikas, "Bounded nonlinear stabilizing speed regulators for VSI-Fed induction motors in field-oriented operation," *IEEE Trans. Control Syst. Technol.*, vol. 22, no. 3, pp. 1112–1121, May 2014.
[34] N. Mohan, T. M. Underland, and W. P. Robbins, *Power Electronics*. Hoboken, NJ, USA: Wiley, 2003.
[35] J.-J. E. Slotine and W. LI, *Applied Nonlinear Control*. Englewood Cliffs, NJ, USA: Prentice-Hall, 1991.
[36] H. K. Khalil, *Nonlinear Systems*. Englewood Cliffs, NJ, USA: Prentice-Hall, 2001.
[37] E. D. Sontag, "Smooth stabilization implies coprime factorization," *IEEE Trans. Autom. Control*, vol. 34, no. 4, pp. 435–443, Apr. 1989.

Antonio T. Alexandridis (M'88) received the Diploma degree in electrical engineering from the Department of Electrical Engineering, University of Patras, Rion, Greece, in 1981, and the Ph.D. degree in electrical engineering from the Department of Electrical and Computer Engineering, West Virginia University, Morgantown, WV, USA, in 1987.

He joined the Department of Electrical and Computer Engineering, University of Patras, in 1988, where he is currently a Professor and the Head of the Power Systems Division. During 1998, he joined the Control Engineering Research Centre, City University London, London, U.K., as a Visiting Researcher. He has authored more than 130 international journal and conference papers. His research interests include control theory, nonlinear dynamics, optimal control, eigenstructure assignment, passivity, and advanced control applications on power systems and drive systems. His current research interests include renewable power generation control and stability (wind generators, PV systems, and microgrids).

Prof. Alexandridis is a Member of the National Technical Chamber of Greece.

George C. Konstantopoulos (S'07–M'13) received the Diploma and Ph.D. degrees in electrical and computer engineering from the Department of Electrical and Computer Engineering, University of Patras, Rion, Greece, in 2008 and 2012, respectively.

He has been with the Department of Automatic Control and Systems Engineering, University of Sheffield, Sheffield, U.K., since 2013, where he is currently a Research Fellow. His current research interests include nonlinear modeling, control, and stability analysis of power converter and electric machine systems with an emphasis in microgrid operation, renewable energy systems, and motor drives.

Dr. Konstantopoulos is a Member of the National Technical Chamber of Greece.

Qing-Chang Zhong (M'03–SM'04) received the Ph.D. degree in control theory and engineering from Shanghai Jiao Tong University, Shanghai, China, in 2000, and the Ph.D. degree in control and power engineering from Imperial College London, London, U.K., in 2004.

He holds the Max McGraw Endowed Chair Professor in Energy and Power Engineering at the Illinois Institute of Technology, Chicago, IL, USA, and a Research Chair at the University of Sheffield, Sheffield, U.K. He (co-)authored three research monographs, including *Control of Power Inverters in Renewable Energy and Smart Grid Integration* (Wiley, 2013) and *Robust Control of Time-delay Systems* (Springer, 2006), and proposed the architecture for next-generation smart grids to unify the interface of all players with the grid through the synchronisation mechanism of conventional synchronous machines. His research interests include advanced control theory and its applications to various sectors including power and energy engineering, chemical engineering, and mechatronics.

Prof. Zhong is a Distinguished Lecturer of the IEEE Power Electronics Society, and is the U.K. Representative to the European Control Association. He serves as an Associate Editor for IEEE TRANSACTIONS ON AUTOMATIC CONTROL/POWER ELECTRONICS/INDUSTRIAL ELECTRONICS/CONTROL SYSTEMS TECHNOLOGY, IEEE ACCESS, IEEE JOURNAL OF EMERGING AND SELECTED TOPICS IN POWER ELECTRONICS, and the *European Journal of Control*.